

Supplemental material:

Table S1: Log₁₀ mutation frequencies at 12 and 20 mg/L (3x and 5x the baseline MIC) piperacillin and 2.5 and 5 mg/L (3x and 5x the baseline MIC) tobramycin at various time points for each dosage regimen simulated (creatinine clearance = 250 mL/min) in the HFIM.^a

	Time (h)	Control	PIP 4 g q4h	TOB 5 mg/kg q24h	TOB 7 mg/kg q24h	TOB 10 mg/kg q48h	PIP 4 g q4h + TOB 5 mg/kg q24h	PIP 4 g q4h + TOB 7 mg/kg q24h	PIP 4 g q4h + TOB 10 mg/kg q48h
12 mg/liter PIP (3x MIC)	0	< -6.33	< -6.33	< -6.33	< -6.33	< -6.33	< -6.33	< -6.33	< -6.33
	23	-4.59	-2.53	-	-	-	< 0.7	< 0.7	< 0.7
	47	< -9.41	-4.13	-	-	-	< 0.7	< -0.3	< 0.7
	95	< -9.51	-2.49	-	-	-	< 0.7	< 0.7	< 0.7
	143	-4.48	-2.60	-	-	-	< -3.24	< -3.12	< -3.13
	191	-3.52	-2.66	-	-	-	< -3.02	< 0.7	< 0.7
20 mg/liter PIP (5x MIC)	0	< -6.33	< -6.33	< -6.33	< -6.33	< -6.33	< -6.33	< -6.33	< -6.33
	23	-4.37	-3.27	-	-	-	< 0.7	< 0.7	< 0.7
	47	-4.64	-3.89	-	-	-	< 0.7	< -0.3	< 0.7
	95	-4.66	-3.55	-	-	-	< 0.7	< 0.7	< 0.7
	143	-4.64	-3.14	-	-	-	< -3.24	< -3.12	< -3.13
	191	-6.15	-4.15	-	-	-	< -3.02	< 0.7	< 0.7
2.5 mg/liter TOB (5x MIC)	0	< -6.33	< -6.33	< -6.33	< -6.33	< -6.33	< -6.33	< -6.33	< -6.33
	23	-6.68	-	-5.93	< -2.58	< -1.83	< 0.7	< 0.7	< 0.7
	47	-6.73	-	-5.04	-7.25	-0.49	< 0.7	< -0.3	< 0.7
	95	-6.97	-	-2.61	-2.16	-1.63	< 0.7	< 0.7	< 0.7
	143	-6.05	-	-3.33	-1.55	-1.54	-1.59	-2.64	-2.36
	191	-7.28	-	-3.02	-3.19	-3.24	< -3.02	< 0.7	< 0.7

	0	< -6.33	< -6.33	< -6.33	< -6.33	< -6.33	< -6.33	< -6.33	< -6.33
5 mg/liter	23	-7.62	-	< -6.24	< -2.58	< -1.83	< 0.7	< 0.7	< 0.7
TOB (10x	47	-7.94	-	-5.28	-7.55	-1.46	< 0.7	< -0.3	< 0.7
MIC)	95	-7.87	-	-3.06	-3.72	-2.10	< 0.7	< 0.7	< 0.7
	143	-6.56	-	-4.85	-3.73	-3.91	< -3.24	< -3.12	< -3.13
	191	-7.68	-	-4.62	-4.69	-4.72	< -3.02	< 0.7	< 0.7

^a When no colonies were present on antibiotic-containing plates, mutation frequencies reported represent an upper limit based on the total viable count.

-: Viable counts on these antibiotic-containing plates were not assessed for the respective regimen.

Table S2. MIC values from colonies obtained from drug-containing agar plates (piperacillin at 12 and 20 mg/liter, equivalent to 3x and 5xMIC; tobramycin at 2.5 and 5 mg/liter, equivalent to 5x and 10xMIC) before treatment (0h) and at various time points for each dosage regimen simulated in the HFIM.

Treatment	Time (h)	Piperacillin		Time (h)	Tobramycin	
		12 mg/liter	20 mg/liter		2.5 mg/liter	5.0 mg/liter
Control	0	16	8	0	8	-
	143	8	8	143	8	-
	191	8	8	191	4	-
PIP 4 g q4h	143	32	64	.	.	.
	191	32	64	.	.	.
TOB 5 mg/kg q24h	.	.	.	143	8	8
	.	.	.	191	8	8
TOB 7 mg/kg q24h	.	.	.	143	8	16
	.	.	.	191	8	16
TOB 10 mg/kg q48h	.	.	.	143	8	8
	.	.	.	191	8	8
PIP 4 g q4h + TOB 5 mg/kg q24h	143	-	-	143	8	-
	191	-	-	191	-	-
PIP 4 g q4h + TOB 7 mg/kg q24h	143	-	-	143	8	-
	191	-	-	191	-	-
PIP 4 g q4h + TOB 10 mg/kg q48h	143	-	-	143	8	-
	191	-	-	191	-	-

-, no colonies on antibiotic-containing plates. PIP, piperacillin; TOB, tobramycin. The EUCAST MIC breakpoints were 16 mg/liter for piperacillin/tazobactam and 4 mg/liter for tobramycin.

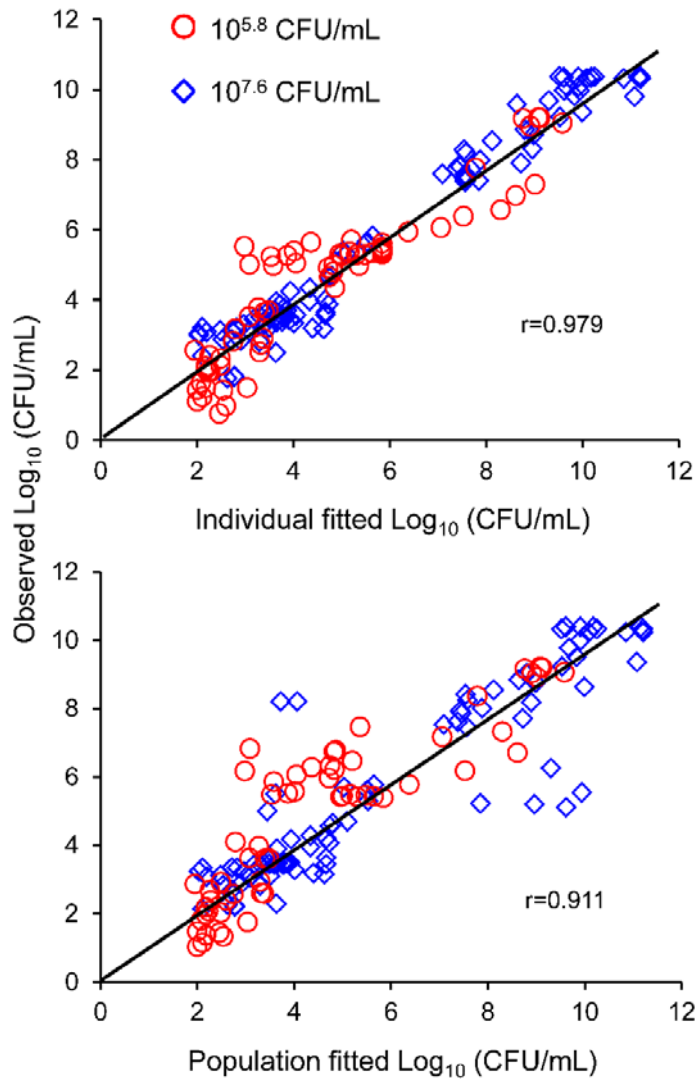


Fig. S1: Observed *versus* individual fitted (top) and population fitted (bottom) viable counts for piperacillin and tobramycin alone and in combinations in SCKT.

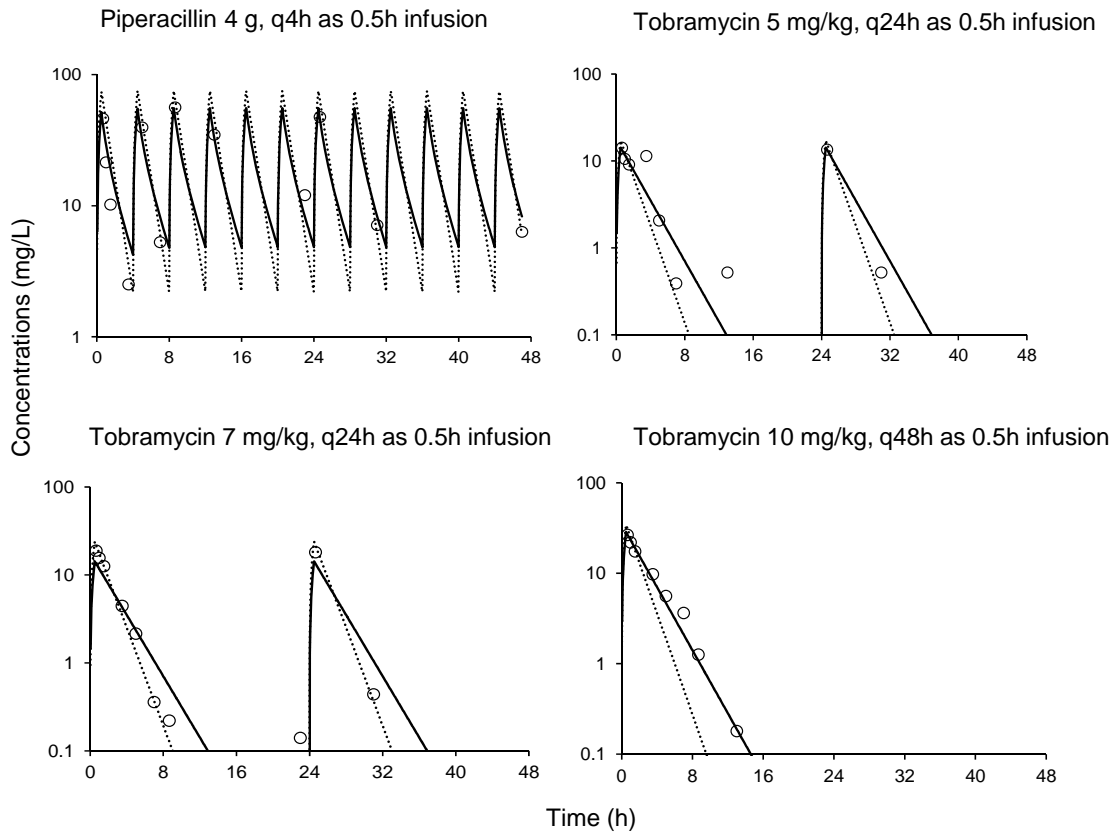


Figure S2: Typical simulated pharmacokinetic profiles showing the relationship between targeted (broken lines), measured (symbols) and model fitted (continuous lines) concentrations of piperacillin and tobramycin in the HFIM.

Mechanism-based population PK/PD modeling

Mechanism-based modeling (MBM) of SCKT data at both inocula was performed utilizing S-ADAPT (version 1.57, importance sampling, pmethod=4) (1, 2) and SADAPT-TRAN (1, 2). Competing models were evaluated based on the biological plausibility of the parameter estimates, the S-ADAPT objective function value ($-1 \times \log$ -likelihood), standard diagnostic plots, the coefficient of correlation and visual predictive checks (3-6).

A life-cycle growth model was utilized to describe the underlying biology of bacterial replication (7, 8). The first-order growth rate constant (k_{12}) determines the mean generation time (MGT) and reflects the transition from the vegetative state (*i.e.* state 1) to the replication state (*i.e.* state 2). The k_{21} was set to 50h^{-1} , since replication was assumed to be fast (8). Models with two and three bacterial subpopulations that described the antibiotic effects *via* direct bacterial killing and inhibition of successful replication by piperacillin were considered. The final model for the combinations included three pre-existing subpopulations of different susceptibility to piperacillin and tobramycin (**Figure 1**). Each population was described in the two states (*i.e.* compartments) mentioned above. The total concentration of viable bacteria (CFU_{all}) was:

$$\text{CFU}_{\text{all}} = \text{CFU}_{\text{SS1}} + \text{CFU}_{\text{SS2}} + \text{CFU}_{\text{R11}} + \text{CFU}_{\text{R12}} + \text{CFU}_{\text{IR1}} + \text{CFU}_{\text{IR2}} \quad (1)$$

The $\text{CFU}_{\text{NN\#}}$ described the concentration of viable bacteria for population NN in state 1 or 2. The effect of piperacillin on inhibition of the probability of successful replication, denoted Inh_{REP} , was described as (9).

$$\text{Inh}_{\text{REP}} = \left(\frac{I_{\text{max,REP}} \cdot C^{\text{Hill,REP}}}{C^{\text{Hill,REP}} + \text{IC}_{50,\text{REP}}} \right) \quad (2)$$

where $I_{\text{max,REP}}$ is the maximum inhibition of the probability of successful replication, $\text{IC}_{50,\text{REP}}$ the concentration causing 50% of the maximum inhibition effect and $\text{Hill}_{,\text{REP}}$ the Hill coefficient, which describes the steepness of the concentration-effect relationship. Two different $\text{IC}_{50,\text{REP}}$ parameters are required ($\text{IC}_{50,\text{SS,REP}}$ and $\text{IC}_{50,\text{IR,REP}}$). An Inh_{REP} of 0.50 results in net stasis of the respective bacterial population and an Inh_{REP} of >0.50 results in bacterial killing, since bacteria that replicate unsuccessfully are eliminated.

The differential equation for the double susceptible population in state 1 (CFU_{SS1}) included killing by piperacillin (C_{PIP} ; piperacillin concentration) and tobramycin (C_{TOB} ; tobramycin concentration) (initial conditions described below):

$$\frac{d(\text{CFU}_{\text{SS1}})}{dt} = 2 \cdot \text{PLAT} \cdot (1 - \text{Inh}_{\text{REP}}) \cdot k_{21} \cdot \text{CFU}_{\text{SS2}} - k_{12,\text{SS}} \cdot \text{CFU}_{\text{SS1}} - \left(\frac{K_{\text{max PIP}} \cdot C_{\text{PIP}}^{\text{Hill PIP}}}{C_{\text{PIP}}^{\text{Hill PIP}} + K_{\text{C}_{50,\text{SS,PIP}}}} + \frac{K_{\text{max SS,TOB}} \cdot C_{\text{TOB}}}{C_{\text{TOB}} + K_{\text{C}_{50,\text{SS,TOB}}}} \right) \cdot \text{CFU}_{\text{SS1}} \quad (3)$$

The CFU_{SS2} is the bacterial concentration of the double susceptible population in state 2. The plateau factor (PLAT) represents the probability of successful replication and is defined as described previously (10, 11). The maximum killing rate constant (K_{max}), the associated antibiotic concentrations ($K_{\text{C}_{50}}$) causing 50% of K_{max} and the Hill coefficient (Hill_{PIP}) for piperacillin are illustrated in **Figure 1** and **Table 1**. Killing by piperacillin and tobramycin was assumed to affect both states and thus the same killing terms were included for states 1 and 2. The double susceptible population in state 2 (CFU_{SS2}) was described as:

$$\frac{d(\text{CFU}_{\text{SS2}})}{dt} = -k_{21} \cdot \text{CFU}_{\text{SS2}} + k_{12, \text{SS}} \cdot \text{CFU}_{\text{SS1}} - \left(\frac{K_{\text{max, PIP}} \cdot C_{\text{PIP}}^{\text{Hill}_{\text{PIP}}}}{C_{\text{PIP}}^{\text{Hill}_{\text{PIP}}} + \text{KC}_{50, \text{SS, PIP}}} + \frac{K_{\text{max, SS, TOB}} \cdot C_{\text{TOB}}}{C_{\text{TOB}} + \text{KC}_{50, \text{SS, TOB}}} \right) \cdot \text{CFU}_{\text{SS2}} \quad (4)$$

The differential equations for the other two populations (RI and IR) were similar but included different estimates for K_{max} , KC_{50} and k_{12} compared to the double susceptible population.

Mechanism-based modeling of synergy: In this modeling analysis we evaluated two types of synergistic interactions: 1) subpopulation synergy (*i.e.* antibiotic A killing the bacteria resistant to antibiotic B and *vice versa*) and 2) mechanistic synergy (*i.e.* antibiotic A enhancing the killing by antibiotic B against one or multiple bacterial populations) (12-14). Mechanistic synergy was incorporated in the model assuming that disruption of the bacterial outer membrane by tobramycin increases the target site penetration of piperacillin (12-14). This permeabilizing effect of tobramycin was implemented in the model *via* the term OM_effect (13, 14). (parameters explained in **Table 1**):

$$\text{OM_effect} = 1 - \left(\frac{I_{\text{max, OM, TOB}} \cdot C_{\text{TOB}}}{C_{\text{TOB}} + \text{IC}_{50, \text{OM, TOB}}} \right) \quad (5)$$

Between-curve variability was set to 10% coefficient of variation during the end of the estimation (15). The \log_{10} viable counts were fitted using an additive residual error model. For observations below 100 CFU/mL (equivalent to fewer than 10 colonies per plate), a previously developed residual error model was utilized to fit the number of colonies per plate (15).

References:

1. Bulitta JB, Bingolbali A, Shin BS, Landersdorfer CB. 2011. Development of a new pre- and post-processing tool (SADAPT-TRAN) for nonlinear mixed-effects modeling in S-ADAPT. *AAPS J* 13:201-211.
2. Bulitta JB, Landersdorfer CB. 2011. Performance and robustness of the Monte Carlo importance sampling algorithm using parallelized S-ADAPT for basic and complex mechanistic models. *AAPS J* 13:212-226.
3. Bulitta JB, Duffull SB, Kinzig-Schippers M, Holzgrabe U, Stephan U, Drusano GL, Sorgel F. 2007. Systematic comparison of the population pharmacokinetics and pharmacodynamics of piperacillin in cystic fibrosis patients and healthy volunteers. *Antimicrob Agents Chemother* 51:2497-2507.
4. Bulitta JB, Zhao P, Arnold RD, Kessler DR, Daifuku R, Pratt J, Luciano G, Hanauske AR, Gelderblom H, Awada A, Jusko WJ. 2009. Mechanistic population pharmacokinetics of total and unbound paclitaxel for a new nanodroplet formulation versus Taxol in cancer patients. *Cancer Chemother Pharmacol* 63:1049-1063.
5. Landersdorfer CB, Kirkpatrick CM, Kinzig-Schippers M, Bulitta JB, Holzgrabe U, Drusano GL, Sorgel F. 2007. Population pharmacokinetics at two dose levels and pharmacodynamic profiling of flucloxacillin. *Antimicrob Agents Chemother* 51:3290-3297.
6. Tsuji BT, Okusanya OO, Bulitta JB, Forrest A, Bhavnani SM, Fernandez PB, Ambrose PG. 2011. Application of pharmacokinetic-pharmacodynamic modeling and the justification of a novel fusidic acid dosing regimen: raising Lazarus from the dead. *Clin Infect Dis* 52 Suppl 7:S513-519.
7. Bulitta JB, Ly NS, Yang JC, Forrest A, Jusko WJ, Tsuji BT. 2009. Development and qualification of a pharmacodynamic model for the pronounced inoculum effect of ceftazidime against *Pseudomonas aeruginosa*. *Antimicrob Agents Chemother* 53:46-56.
8. Maidhof H, Johannsen L, Labischinski H, Giesbrecht P. 1989. Onset of penicillin-induced bacteriolysis in staphylococci is cell cycle dependent. *J Bacteriol* 171:2252-2257.
9. Bergen PJ, Bulitta JB, Kirkpatrick CM, Rogers KE, McGregor MJ, Wallis SC, Paterson DL, Lipman J, Roberts JA, Landersdorfer CB. 2016. Effect of different renal function on antibacterial effects of piperacillin against *Pseudomonas aeruginosa* evaluated via the hollow-fibre infection model and mechanism-based modelling. *J Antimicrob Chemother* 71:2509-2520.
10. Landersdorfer CB, Ly NS, Xu H, Tsuji BT, Bulitta JB. 2013. Quantifying subpopulation synergy for antibiotic combinations via mechanism-based modeling and a sequential dosing design. *Antimicrob Agents Chemother* 57:2343-2351.
11. Yadav R, Landersdorfer CB, Nation RL, Boyce JD, Bulitta JB. 2015. Novel approach to optimize synergistic carbapenem-aminoglycoside combinations against carbapenem-resistant *Acinetobacter baumannii*. *Antimicrob Agents Chemother* 59:2286-2298.
12. Bulitta JB, Ly NS, Landersdorfer CB, Wanigaratne NA, Velkov T, Yadav R, Oliver A, Martin L, Shin BS, Forrest A, Tsuji BT. 2015. Two mechanisms of killing of *Pseudomonas aeruginosa* by tobramycin assessed at multiple inocula via mechanism-based modeling. *Antimicrob Agents Chemother* 59:2315-2327.

13. Yadav R, Bulitta JB, Nation RL, Landersdorfer CB. 2017. Optimization of Synergistic Combination Regimens against Carbapenem- and Aminoglycoside-Resistant Clinical *Pseudomonas aeruginosa* Isolates via Mechanism-Based Pharmacokinetic/Pharmacodynamic Modeling. *Antimicrob Agents Chemother* 61:e01011-16.
14. Yadav R, Bulitta JB, Schneider EK, Shin BS, Velkov T, Nation RL, Landersdorfer CB. 2017. Aminoglycoside concentrations required for synergy with carbapenems against *Pseudomonas aeruginosa* determined via mechanistic studies and modeling. *Antimicrob Agents Chemother* 61:e00722-17.
15. Bulitta JB, Yang JC, Yohonn L, Ly NS, Brown SV, D'Hondt RE, Jusko WJ, Forrest A, Tsuji BT. 2010. Attenuation of colistin bactericidal activity by high inoculum of *Pseudomonas aeruginosa* characterized by a new mechanism-based population pharmacodynamic model. *Antimicrob Agents Chemother* 54:2051-2062.